International Conference on Applied Energy 2019
Aug 12-15, 2019, Västerås, Sweden
Paper ID:405

EXERGETIC ANALYSIS OF THERMAL TRANSPORT IN LATENT HEAT THERMAL ENERGY STORAGE SYSTEMS INFUSED WITH METAL FOAM

Varun Joshi*, Manish K. Rathod
Mechanical Engineering Department, Sardar Vallabhbhai National Institute of Technology, Surat-395007, India

ABSTRACT

A thermal performance of the metal foam-PCM composite (MFPC) infused latent heat thermal energy storage (LHTES) systems are widely evaluated based on the first law of thermodynamics. The thermal performance of such system is, therefore, investigated using the first and second law of thermodynamics during the melting process in a present study. The influence of metal foam porosity on thermal transport is analyzed. Results show that the phase change thermal transport can be improved substantially with an incorporation of the metal foam (ε = 0.97) with the reduction in the melting time by 40% when compared to the pure PCM. A reduction in porosity of metal foam attenuates the high temperature gradients and hence, the entropy generation rate/irreversibility. Subsequently, the steady state exergetic efficiency is found to be 89.20% and 97.87% for the pure PCM and the MFPC respectively.

Keywords: Latent heat thermal energy storage system, Metal foam-PCM composite, Entropy generation number, Exergy efficiency

1. INTRODUCTION

The latent heat thermal energy storage (LHTES) systems with phase change materials (PCMs) has gained a significant attention for the energy conservation due to its large storage density and latent heat of fusion nearly at the isothermal melting temperature. These PCMs are categorized as inorganic, organic, and eutectic combination. The low thermal conductivity of these PCMs, however, affects the energy storage and release rate and leads to the constrained applicability. Therefore, many researchers have proposed various thermal conductivity enhancers (TCE) to alleviate the thermal transport rate [1]. These TCE can be extended surfaces, nano particles, encapsulation, heat pipes, and metallic foams. An open cellular high porosity (above 90%) metal foam has promising attributes such as high thermal conductivity, greater specific surface area contact between the metal foam ligaments and PCM etc. A numerous investigations have been carried out, which often assess the thermal performance of MFPC using an energy balance, where the first law of thermodynamics is generally employed to estimate quantitative techniques to improve the amount of the thermal energy stored and released [2]. The study, however, becomes inadequate when the quality with which it is stored and released when the TES potential is concerned. Bejan [3] quoted that the primary purpose of the thermal energy storage system is not to store the energy, rather to store the useful work. Jagdishwaran et al. [4] presented a lucid review on the thermal performance study of the LHTES system based on the second law. A second law analysis of the shell and tube LHTES was performed by Erek and Dincer [5], which showed that the second law efficiency was significantly lesser than the energy efficiency during the melting process due to the external and internal irreversibilities associated with it. Rathod and Banerjee [6] demonstrated that the entropy generation number was found to be minimized with a higher initial temperature of PCM. Although an extensive research has been carried out on the energy analysis of metal foam infused LHTES systems using the first law of thermodynamics, it is hard to find the literature, which reports an exergetic analysis of such systems. Thereby, there is a need for comprehensive study which estimates exergy destruction in the MFPC infused LHTES system and provides qualitative results for comparison with that of without metal foam.

Thus, the objective of the present study is to present a comprehensive analysis of the metal foam porosity, which influence the melting performance using the first and second law of thermodynamics. An in-house numerical code is developed using a local thermal non-equilibrium (LTNE) equipped enthalpy porosity approach to simulate the enhancement in thermal performance. The outcome of the study depicts that the estimation of the metal foam porosity dependency on exergetic performance can assist in the qualitative selection of the optimum MFPC configuration for the efficient performance of LHTES system.

Selection and peer-review under responsibility of the scientific committee of the 11th Int. Conf. on Applied Energy (ICAE2019).

2. PHYSICAL SYSTEM AND NUMERICAL METHOD

2.1 Domain description

A rectangular LHTES system from an experimental investigation of Zhang et al. [7] is taken into consideration, which comprises copper foam saturated paraffins. The MFPC has a height (*H*), length (*L*), and width (*W*) of 0.1 m x 0.1 m x 0.01 m respectively. The left wall is subjected to a heat flux estimated as 6207.51-0.0108t W/m^2, while the other walls are kept adiabatic. The thermo-physical properties of copper foam and paraffins are adopted from their experimental study [7].

2.2 Governing equations and numerical scheme

A local thermal non-equilibrium supplemented enthalpy porosity approach is invoked owing to non-ignorable attributes, where copper foam and paraffin are at thermal non-equilibrium temperature. The transport equations are as follows.

(a) Continuity equation:

$$\frac{\partial(\rho u)_p}{\partial x}+\frac{\partial(\rho v)_p}{\partial y}=0 \tag{1}$$

(b) X momentum transport equation:

$$\rho_p\left(\frac{\partial u_p}{\partial t}\right)+\frac{\partial(\rho uu)_p}{\partial x}+\frac{\partial(\rho vu)_p}{\partial y}=-\frac{\partial p}{\partial x}+\frac{\partial}{\partial x}\left(\mu_p\frac{\partial u_p}{\partial x}\right)+\frac{\partial}{\partial y}\left(\mu_p\frac{\partial u_p}{\partial y}\right)-A_{mushy}\left(\frac{(1-f)^2}{f^3+z}\right)u_p-\frac{\mu_p}{K}u_p-\frac{1}{\sqrt{K}}C_i\rho_p u_p\sqrt{u_p^2+v_p^2} \tag{2}$$

(c) Y momentum transport equation

$$\rho_p\left(\frac{\partial v_p}{\partial t}\right)+\frac{\partial(\rho uv)_p}{\partial x}+\frac{\partial(\rho vv)_p}{\partial y}=-\frac{\partial p}{\partial x}+\frac{\partial}{\partial x}\left(\mu_p\frac{\partial v_p}{\partial x}\right)+\frac{\partial}{\partial y}\left(\mu_p\frac{\partial v_p}{\partial y}\right)-A_{mushy}\left(\frac{(1-f)^2}{f^3+z}\right)v_p-\frac{\mu_p}{K}v_p-\frac{1}{\sqrt{K}}C_i\rho_p v_p\sqrt{u_p^2+v_p^2}+\rho_p g\beta(T_p-T_{ref}) \tag{3}$$

(d) Thermal energy transport equation: paraffins

$$\varepsilon(\rho C_p)_p\left(\frac{\partial T_p}{\partial t}\right)+\frac{\partial(\varepsilon\rho C_p uT)_p}{\partial x}+\frac{\partial(\varepsilon\rho C_p vT)_p}{\partial y}=\frac{\partial}{\partial x}\left(\left(k_{pe}+k_{td}\right)\frac{\partial T_p}{\partial x}\right)+\frac{\partial}{\partial y}\left(\left(k_{pe}+k_{td}\right)\frac{\partial T_p}{\partial y}\right)-\varepsilon L_h\rho_p\frac{\partial f}{\partial t}+h_{cup}A_{cup}(T_{cu}-T_p) \tag{4}$$

(e) Thermal energy transport equation: copper foam

$$(1-\varepsilon)(\rho C_p)_{cu}\left(\frac{\partial T_{cu}}{\partial t}\right)=\frac{\partial}{\partial x}\left(k_{cue}\frac{\partial T_{cu}}{\partial x}\right)+\frac{\partial}{\partial y}\left(k_{cue}\frac{\partial T_{cu}}{\partial y}\right)+h_{cul}A_{cul}(T_p-T_{cu}) \tag{5}$$

Here, *u* and *v* are liquid PCM velocity, *p* is liquid pressure. The independent variable, ρ is density, *t* is time, μ is dynamic viscosity, *K* is permeability, C_i is inertia coefficient, β is a volumetric thermal expansion coefficient, T_{ref} is a reference temperature. T_p is paraffin temperature and *f is* liquid fraction. T_{cu} is temperature of the metal foam. L_h is latent heat of fusion, ε is the metal foam porosity, C_p is specific heat, k_{pe} and k_{cu} are an effective thermal conductivity of PCM and metal foam respectively, is thermal conductivity due to dispersion, h_{cup} is an interstitial heat transfer coefficient, and A_{cup} is interfacial surface area. The detailed description of these parameters are available in a reference [8]. The subscript *cu* denotes copper foam. The subscript *p* denotes paraffins.

The volume rate of local entropy generation ($S''_{gen,local}$) can be expressed as follows.

$$S'''_{gen,local}=\frac{k_{pe}}{T_0^2}\left[\left(\frac{\partial T_p}{\partial x}\right)^2+\left(\frac{\partial T_p}{\partial y}\right)^2\right]+\frac{\mu_p}{T_0}\left(2\left[\left(\frac{\partial u_p}{\partial x}\right)^2+\left(\frac{\partial v_p}{\partial y}\right)^2\right]+\left(\frac{\partial u_p}{\partial y}+\frac{\partial v_p}{\partial x}\right)^2\right) \tag{6}$$

The global entropy generation rate can be evaluated by integrating over a volume (V),

$$S'''_{global}=\int S'''_{gen,local}\,dV \tag{7}$$

Thereby, the entropy generation number (N_s) and second law efficiency (η_{II}) can be estimated as,

$$N_S=\left(\frac{T_0 S'''_{global}}{Ex_{in}}\right) \tag{8}$$

$$\eta_{II}=1-N_S \tag{9}$$

Here, T_0 is a surrounding temperature and Ex_{in} is exergy supplied during melting process.

A 2D rectangular domain (0.1 m x 0.1 m) is discretized using finite volume method. The semi-implicit pressure linked equations (SIMPLE) is employed to obtain the velocity and pressure field. An enthalpy porosity formulation is used to obtain the temperature

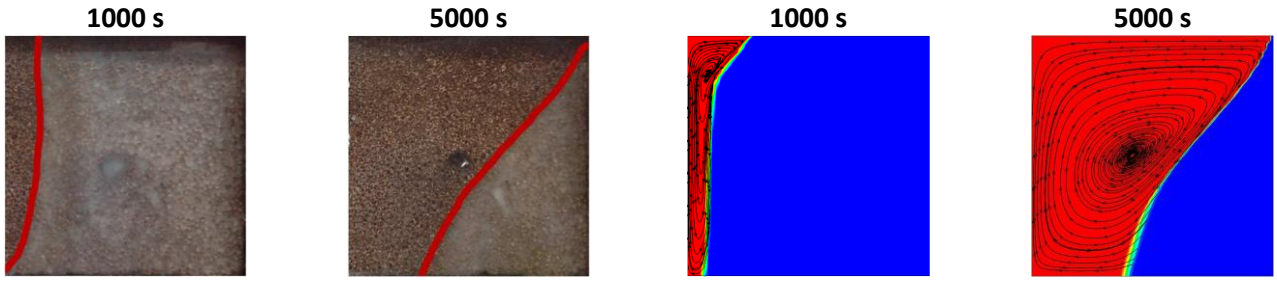

(a) An experimental study, Zhang et al. [6] (b) A present numerical study

Figure 1: Comparison between the developement of the liquid-solid interface contours during the experimental investigation (Zhang et al. [6]) and the present numerical study during the melting process

field and the liquid fraction of PCM while the thermal energy transport equation is solved for the metal foam separately. The developed numerical code is fully implicit in time and advection terms are handled by quadratic upstream interpolation for convective kinematics (QUICK) scheme. The discretized equations are solved by an iterative procedure using Gauss-Seidel successive over-relaxation (GS-SOR) algorithm. If the relative difference in these variables is less than 10^{-6} times of their initial values, then the solution is declared to be converged. The optimum grid size of 10,000 cells with a time step of 0.001 s are utilized due to the achievement of sufficient defined convergence.

2.3 Validation

Figure 1 shows the comparison of the evolvement of the liquid-solid interface contours during the experimental expedition [6] and the present numerical study at the various time intervals during the melting process. A well agreement with the experimental results can be observed from the overall positions and morphology of the liquid-solid interfaces in the present numerical study.

3. RESULTS AND DISCUSSION

The aforementioned numerical approach is employed to investigate the influence of the variation in the porosity (from 0.97 to 0.90) on the melting performance. The temporal variation in the average melt volume fractions for the configuration with ε = 0.97 (Configuration 1), for the configuration with ε = 0.95 (Configuration 2), for the configuration with ε = 0.92 (Configuration 3), and for the configuration with ε = 0.90 (Configuration 4) are shown in Figure 2. The case with the pure PCM (paraffins) is referred as Configuration 0. It can be observed that the pure PCM shows the poor melting rate among all the configurations due to the low thermal conductivity. The time require to melt pure PCM is observed to be 15000 s. A profound influence of metal foam on the melting process can be seen in Configuration 1 to 4 when compared to Configuration 0 due to high effective thermal conductivity ligaments. The linearity in the curves explains the intensive conductive transport, which decreases the thermal resistances, and hence, the high temperature gradients. The total melting time required, therefore, in Configuration 1, 2, 3, and 4 to melt paraffins is 9000 s, 7000 s, 6000 s, and 5000 s respectively.

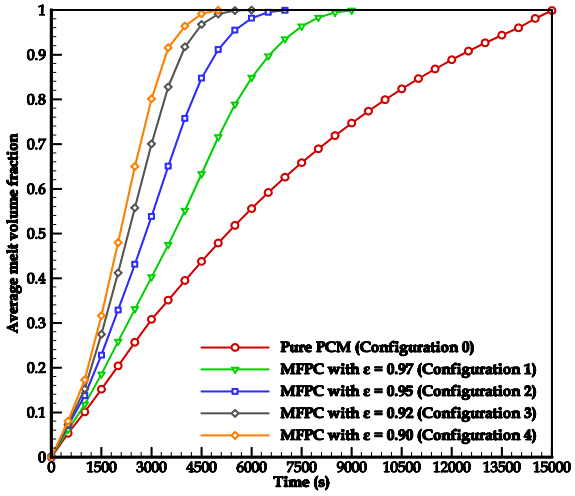

Figure 2. Time series of the average melt volume fraction

The temporal variation in the volumetric entropy generation ($S^{"}_{gen,\mathrm{local}}$) for all the configurations during the melting process is shown in Figures 3. It can be observed that $S^{"}_{gen,local}$ is maximum during the initial period of the melting process of the pure PCM. This can be attributed to the high temperature gradients exist in the low temperature pure PCM. After 1000 s, the temporal variation of the entropy generation commences to increase gradually due to a reduction in local temperature gradients and rise in the temperature of the PCM. Further, it can be seen that the entropy generation rate is lower in the case of the MFPC with ε = 0.97 when compared to the pure PCM. This can be credited to the high thermal conductivity metal foam

ligaments, which increases the effective thermal conductivity. The low entropy generation rates indicate uniform temperature distribution hence, the lower temperature gradients/thermal resistances and more rapid the melting process. Furthermore, it can be seen that the increase in the mass of metal (decrease in porosity) attenuates entropy generation rate/irreversibility of LHTES system. The trend of $S''_{gen,local}$ for all the MFPC configurations can observe to be almost identical up to 3000 s when the liquid-solid interface is at the top portion of enclosure. The significant reduction in $S''_{gen,local}$ rate in the Configurations 3 and 4 can be observed post to 3000 s when the liquid-solid interface reaches to the middle portion of enclosure. Further reduction in $S''_{gen,local}$ rate can be observed when the interface in the bottom portion of the enclosure, especially at the culmination stage of the melting process. Hence, it can be concluded that the thermal transport can be augmented by the decrease in the porosity of the metal foam, increases exergy of a system and results in the decrease in irreversibilities.

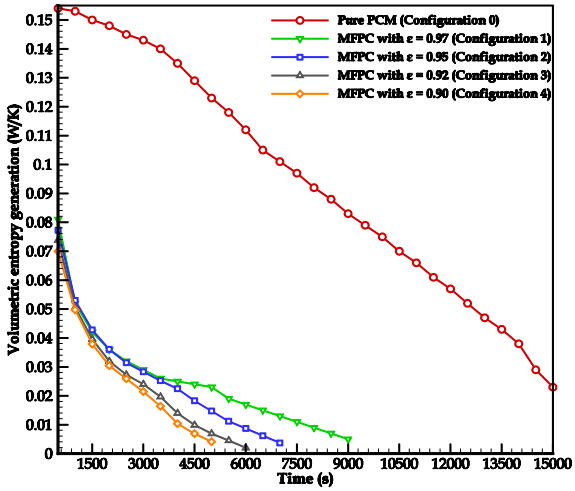

Figure 3. Time series of the volumetric entropy generation

N_s assists to calculate the exergy destruction hence, the loss of the available useful part of energy, which is calculated with the use of a first law of thermodynamics. The exergy input (Ex_{in}) remains equal to flux (6207.51-0.0108t W/m^2) supplied at the left wall of the enclosure. As Ex_{in} is identical, no change in the trajectory of curve can be observed when compared to Figure 3. It has been observed that the N_s is maximum for the pure PCM due to the poor conductive transport and the high temperature gradients. In addition, the decrement in the porosity metal gradually decreases N_s. The N_s for pure PCM is found to be 0.108 at steady state. The lower N_s can be observed in Configuration 4 (i.e. 0.0071), while Configuration 3 (i.e. 0.014), 2 (i.e. 0.0177), and 1 (0.0211) stand next to it. A corresponding η_{II} for Configuration 0, 1, 2, 3, and 4 are found to be 89.20%, 97.87%, 98.23%, 98.6%, and 99.29% respectively.

4. CONCLUSION

An exergetic analysis of metal foam associated LHTES system is carried out. The influence of porosity on the entropy generation and exergy efficiency is estimated and compared with that of pure PCM. The results show that the variation in porosity significantly affects the entropy generation rate and overall melting performance. The exergy efficiency is found to be increased (with a reduction in entropy generation) with a decrease in the metal foam porosity. The maximum exergetic efficiency is observed for the porosity of 0.90 among given configurations, which can be attributed to maximum metal mass inclusion (higher effective thermal conductivity).

References

[1] Fan L, Khodadadi JM. Thermal conductivity enhancement of phase change materials for thermal energy storage: a review. Renewable and sustainable energy reviews. 2011 Jan 1;15(1):24-46.

[2] Joshi V, Rathod MK. Constructal enhancement of thermal transport in metal foam-PCM composite-assisted latent heat thermal energy storage system. Numerical Heat Transfer, Part A: Applications. 2019 Mar 19;75(6):413-33.

[3] Bejan A. Entropy generation minimization: the method of thermodynamic optimization of finite-size systems and finite-time processes. CRC press; 2013 Oct 29.

[4] Jegadheeswaran S, Pohekar SD, Kousksou T. Exergy based performance evaluation of latent heat thermal storage system: a review. Renewable and Sustainable Energy Reviews. 2010 Dec 1;14(9):2580-95.

[5] Erek A, Dincer I. A new approach to energy and exergy analyses of latent heat storage unit. Heat Transfer Engineering. 2009 May 1;30(6):506-15.

[6]Rathod MK, Banerjee J. Entropy generation assessment of shell and tube latent heat storage unit. International Journal of Exergy. 2015 Jan 1;16(1):97-108.

[7] Zhang P, Meng ZN, Zhu H, Wang YL, Peng SP. Melting heat transfer characteristics of a composite phase change material fabricated by paraffin and metal foam. Applied energy. 2017 Jan 1;185:1971-83.

[8] Joshi V, Rathod MK. Thermal transport augmentation in latent heat thermal energy storage system by partially filled metal foam: A novel configuration. Journal of Energy Storage. 2019 Apr 1;22:270-82.